



ELSEVIER

Physica B 314 (2002) 230–234

PHYSICA B

www.elsevier.com/locate/physb

Application of narrow band-gap materials in nanoscale spin filters

M.J. Gilbert^a, J.P. Bird^{a,*}, T. Sugaya^b, R. Akis^a

^a Department of Electrical Engineering and Center for Solid State Electronics Research, Arizona State University, Tempe, AZ 85287-5706, USA

^b National Institute of Advanced Industrial Science and Technology (AIST), 1-1-4, Umezono, Tsukuba 305-8568, Japan

Abstract

We develop a simple analytical model to study the influence of different material systems on the operation of a quantum-point-contact spin filter. Such a device has been predicted to allow for local control of the spin polarization in a semiconductor, and for direct electrical detection of the induced spin polarization. Narrow band-gap semiconductors, such as InAs and InSb, are predicted to exhibit excellent spin-filter characteristics, due to their large g -factor values, and enhanced subband splittings. As a practical step towards the realization of such a spin filter, the electrical properties of InGaAs quantum wires are investigated. © 2002 Elsevier Science B.V. All rights reserved.

PACS: 73.23.–b; 73.23.Ad; 85.30.Vw; 72.20.–i

Keywords: Spintronics; Spin filter; Quantum point contact

1. Introduction

The possibility of exploiting the spin degree of freedom of charge carriers in novel electronic devices is currently an area of research that is attracting considerable experimental and theoretical interest [1–3]. In many of these *spintronic* applications, an *electrical* means for both generating and detecting spin-polarized distributions of carriers is desired. Motivated by these requirements, we have previously [4,5] proposed a design for a tunable spin filter that exploits the known transmission properties of ballistic quantum wires

to generate spin-polarized carriers. In this report, we consider the influence of different material systems on the practical operation of this spin filter. In order to successfully implement such a device, we argue that quantum wires with a large separation of their one-dimensional subbands, and a strongly enhanced effective g -factor, will be required. The first requirement is necessary to ensure that the filtering action involves *only* the lowest subband of the wire, while the second allows effective spin filtering to be achieved at lower magnetic fields, and higher temperatures. As a step towards the practical realization of the spin-filter structure, we present the results of recent studies of the transport properties of InGaAs quantum wires [6], which are found to exhibit the desired one-dimensional transport characteristics.

*Corresponding author. Tel.: +1-480-965-7421; fax: +1-480-965-8058.

E-mail address: bird@asu.edu (J.P. Bird).

2. Theoretical model

Since the basic principles of the spin-filter device have been described in detail elsewhere [4,5], in this section we briefly summarize the key features of its operation. The basic device structure is shown in Fig. 1 and consists of a multi-layered gate structure that is deposited on the surface of a high-mobility heterojunction. The lower set of split gates is used to define a quantum point contact in the two-dimensional electron gas of the heterojunction, while the upper, continuous, gate is separated from the lower gates by an insulating layer. In basic operation, the split gates are configured to set the point contact close to its conduction threshold. A steady current is then driven through the upper gate, inducing a local magnetic field that lifts the spin degeneracy of the carriers and causes preferential transmission of one spin species through the point contact. To develop an analytical model of the spin-filter operation, we assume that the potential barrier generated by the point contact exhibits a two-dimensional parabolic form. In the presence of a perpendicular magnetic field, the transmission probability of the n th subband may then be written as [7]:

$$T_n = \frac{1}{1 + \exp(-\pi\varepsilon_n)},$$

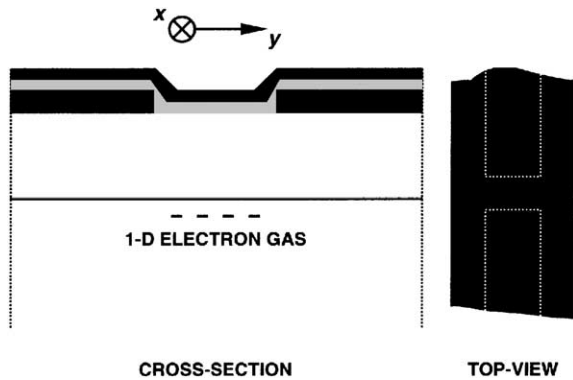


Fig. 1. Schematic illustration of the quantum-point-contact spin filter. Black regions correspond to metallic gates, while the gray shading denotes a thin insulating layer. The coordinate system is also indicated for reference.

$$\varepsilon_n = \frac{E - E_2(n + 1/2) - V_0}{E_1},$$

$$E_1 = \frac{\hbar}{2\sqrt{2}} ([\Omega^4 + 4\omega_x^2\omega_y^2]^{0.5} - \Omega^2)^{0.5}, \quad (1b)$$

$$E_2 = \frac{\hbar}{\sqrt{2}} ([\Omega^4 + 4\omega_x^2\omega_y^2]^{0.5} + \Omega^2)^{0.5}. \quad (1c)$$

Here, ω_x and ω_y are the oscillator frequencies that define the variation of the barrier potential in the directions parallel and perpendicular to the current flow, respectively. V_0 is the saddle-barrier height at the center of the channel, and may be controlled directly in the experiment by means of the split-gate voltage. Ω is a magnetic-field-dependent oscillator frequency ($\Omega^2 = \omega_c^2 - \omega_x^2 + \omega_y^2$) while the cyclotron frequency $\omega_c = eB/m^*$. With these definitions, the response of the spin filter may be computed by introducing the *spin-dependent* transmission probabilities in a magnetic field [4]:

$$T_{\pm} = T_n(E_0 \pm g^* \mu_B B). \quad (2)$$

In Eq. (2), E_0 is the initial electron energy at zero magnetic field and g^* is the effective g -factor of the heterojunction system under study. Since the conductance of the point contact is directly related to these transmission probabilities, a natural advantage of the point-contact spin filter is that a *direct* determination of the spin polarization can be obtained from a measurement of its conductance [4].

To illustrate the basic details of filter action, we have previously considered the response of a GaAs/AlGaAs structure and found that magnetic fields as large as a Tesla should be required to generate satisfactory spin filtration. In Fig. 2, however, we consider the response of a spin filter, realized in the narrow-gap semiconductor InSb. The key differences of this material with GaAs are its large g -factor enhancement ($g^* = -51$), and the small value of its effective mass ($m^* = 0.014m_0$). In Figs. 2(a) and (b), we plot the variation of the two spin-dependent transmission probabilities for an InSb spin filter with realistic barrier parameters. The energy range considered here is chosen to correspond to that over which the conductance of the point contact is dominated by the first subband

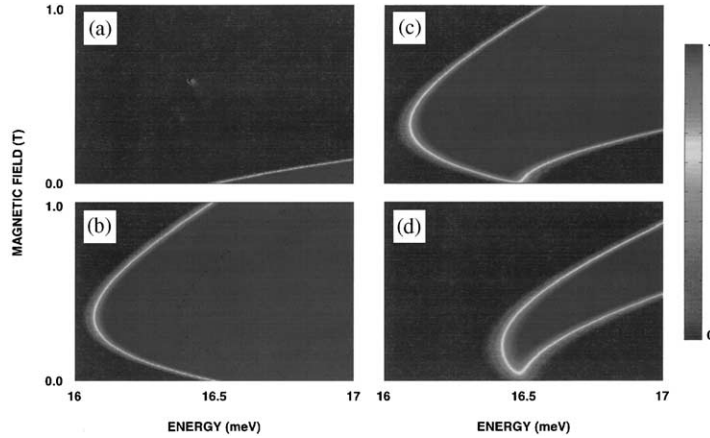


Fig. 2. (a) T_+ versus energy and magnetic field for an InSb spin filter. (b) T_- versus energy and magnetic field for an InSb spin filter. (c) Differential transmission ($T_+ - T_-$) versus energy and magnetic field for an InSb spin filter. (d) Differential transmission ($T_+ - T_-$) versus energy and magnetic field for an InAs spin filter. These calculations are for spin filters with the following parameters: $V_0 = 15$ meV, $\hbar\omega_y = 3$ meV and $\hbar\omega_x = 0.1$ meV. $g^* = -51$ for InSb and -15 for InAs.

($n = 0$) alone. In both of these figures, it is clear that the threshold for conduction through the barrier *increases* with increasing magnetic field, which simply reflects the reduced kinetic energy of the electrons at higher magnetic fields. In Fig. 2(c), the differential transmission probability of the two spins ($T_+ - T_-$) is plotted, and the lighter region now indicates the range of parameter space where the transmission of one spin species is high while that of the other is low. At those energies which lie *below* this range, spin filtering is ineffective since the transmission probability for *both* spin species is essentially zero (see Figs. 3(a) and (b)). Similarly, for those energies that lie *above* this range, spin filtration is equally ineffective since the transmission probability of *both* spins is now close to unity. The crucial feature for the discussion here is the *magnitude* of the magnetic field required to achieve spin polarization. As can be seen from the lighter region in Fig. 2(c), full polarization of the transmitted carriers occurs for a magnetic field as small as a few mT. This dramatically reduced magnetic-field requirement is a direct consequence of the large g -factor enhancement in InSb. As a further illustration of this effect, in Fig. 2(d) we show the corresponding spin-filter characteristic for an InAs-based ($g^* = -15$) structure. In this case a field of a few tens of mT is required to achieve spin

filtration, which higher value results due to the reduced g -factor compared to InSb. Nonetheless, even for magnetic fields of this order, it should be possible to generate the desired spin polarization using a ferromagnetic gate through which magnetizing and demagnetizing current pulses are driven.

While the preceding calculations are performed for zero temperature, the influence of finite temperature on the spin-filter action can be easily accounted for, by convolving the zero-temperature transmission probabilities with the derivative of the Fermi function. To a good approximation, this convolution leads to the temperature-dependent transmission probabilities [8,9]:

$$T_{\pm}(E, B) = \frac{1}{1 + e^{-(E - E_{\pm}^{\pm}(B))/k_B T}}. \quad (3)$$

Here, $E_1^+(B)$ and $E_1^-(B)$ are the turn-on energies of the first, spin-resolved, subbands, which we define as the particular energy at which the zero-temperature transmission increases to 0.5. In Fig. 3, we show the effect of temperature on the spin-filter characteristics of GaAs and InSb devices. At 4.2 K, the spin filtration is lost completely in the GaAs, but still persists in InSb. Once again, these different characteristics reflect the large difference in the spin-splitting energies for these two materials. A problem at these

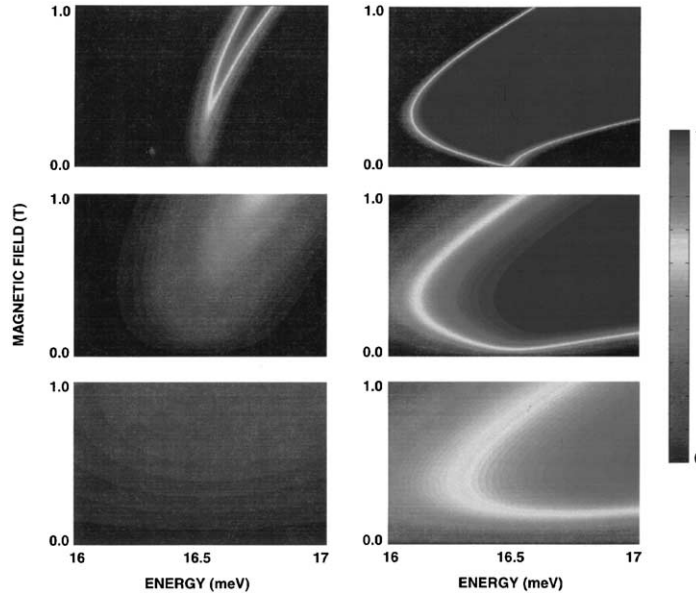


Fig. 3. Temperature dependence of the spin-filter action in two different material systems. The left three contours are for GaAs (we have arbitrarily assumed $g^* = 2$ here) and the right three panels are for InSb. As before, the filter parameters for both systems are $V_0 = 15$ meV, $\hbar\omega_y = 3$ meV and $\hbar\omega_x = 0.1$ meV. The temperature is 0 K for the top panels, 1 K for the center panels, and 4.2 K for the bottom panels.

temperatures, however, is that transport through higher subbands becomes possible. In order to ensure that transport involves only the lowest subband at increased temperatures, it is therefore necessary that the point contact exhibit a large energy splitting ($\hbar\omega_y$) of its transverse subbands.

3. Experimental investigations

The preceding discussion reveals that materials exhibiting a large enhancement of their g -factor, and a large splitting of their subbands in quantum wires, are desired for application in the proposed spin filter. As a first step towards the realization of such a device, we have therefore recently investigated the one-dimensional transport characteristics of $\text{In}_{0.47}\text{Ga}_{0.53}\text{As}$ quantum wires [10]. Our interest in this material system is motivated by a number of factors. The first is the large g -factor this material is expected to exhibit ($g^* \approx -6$), while the second is the small value of the effective mass ($m^* = 0.04m_0$). In quantum wires realized in

this material system, the small value for the mass is expected to result in a large splitting of the one-dimensional subbands, a property we have recently confirmed [6]. In Fig. 4, for example, we show the magneto-resistance of a 300 nm quantum wire that was realized by selective MBE growth on a (100) ridge-type substrate [10]. At magnetic fields in excess of 3 T, the magneto-resistance oscillations result from the depopulation of Landau levels, and exhibit the usual inverse-field periodicity (see upper inset). At lower fields, however, the oscillations deviate from this periodicity, allowing an estimate for the effective width and subband spacing of the wire to be obtained [6,11,12]. By using the gate voltage (see the lower inset) to vary the effective width of the wire, we have obtained subband splittings that range from approximately 3 to 8 meV. This latter value is very much larger than that reported in corresponding studies of GaAs quantum wires [11,12]. In addition to their excellent one-dimensional transport properties, a further advantage of these quantum wires for application in the spin

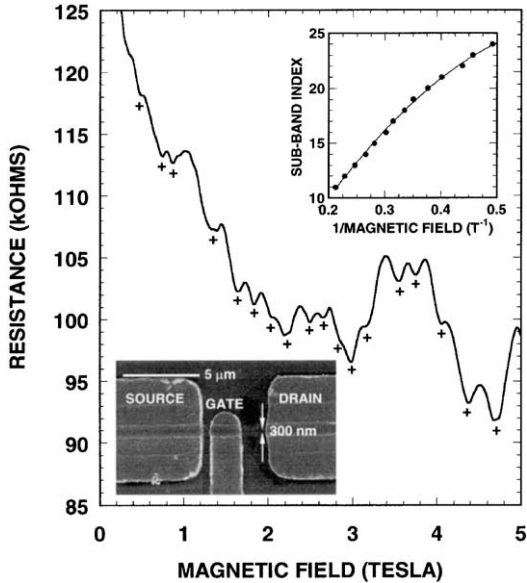


Fig. 4. The magneto-resistance of a 300 nm InGaAs ridge-type quantum wire at 4.2 K. The inset shows an SEM image of the wire, indicating the contact regions and the gate. The upper inset plots the position of the various oscillation minima, identified by the “+” symbols, in the main figure as a function of inverse magnetic field.

filter is the small distance (47 nm) between their surface and the two-dimensional electron gas. This reduced distance should allow for a strong influence of the magnetic-field generating gate and in the future, we therefore, plan to pursue the realization of a spin filter in this high-quality material system.

4. Conclusions

In conclusion, we have developed a simple analytical model to study the influence of different material systems on the operation of a quantum-point-contact spin filter. Such a device has been predicted to allow for local control of the spin

polarization in a semiconductor, and for direct electrical detection of the induced spin polarization. Narrow band-gap semiconductors, such as InAs and InSb, have been predicted to exhibit excellent spin-filter characteristics, due to their large g -factor values, and enhanced subband splittings. As a practical step towards the realization of such devices, the electrical properties of InGaAs quantum wires have been studied and have been found to exhibit much larger one-dimensional subband splittings than equivalent GaAs-based wires.

Acknowledgements

This work was supported by the Office of Naval Research.

References

- [1] S. Datta, B. Das, *Appl. Phys. Lett.* 56 (1990) 665.
- [2] D. Loss, D.P. DiVincenzo, *Phys. Rev. A* 57 (1998) 120.
- [3] G. Burkard, D. Loss, D.P. DiVincenzo, *Phys. Rev. B* 59 (1998) 2070.
- [4] M.J. Gilbert, J.P. Bird, *Appl. Phys. Lett.* 77 (2000) 1050.
- [5] M.J. Gilbert, J.P. Bird, *Technical Proceedings of the Fourth International Conference on Modeling & Simulation of Microsystems*, ISBN 0-9708275-0-4, 2001, pp. 570–573.
- [6] T. Sugaya, M. Ogura, Y. Sugiyama, T. Shimizu, K. Yonei, K.-Y. Jang, J.P. Bird, D.K. Ferry, *Appl. Phys. Lett.* 79 (2001) 371.
- [7] H.A. Fertig, B.I. Halperin, *Phys. Rev. B* 36 (1987) 7969.
- [8] M. Büttiker, Y. Imry, R. Landauer, S. Pinhas, *Phys. Rev. B* 31 (1985) 6207.
- [9] D.K. Ferry, S.M. Goodnick, *Transport in Nanostructures*, Cambridge University Press, Cambridge, 1997, pp. 137–138.
- [10] T. Sugaya, T. Takahashi, T. Nakagawa, M. Ogura, Y. Sugiyama, *Electron. Lett.* 34 (1998) 926.
- [11] K.-F. Berggren, T.J. Thornton, D.J. Newson, M. Pepper, *Phys. Rev. Lett.* 57 (1986) 1769.
- [12] K.F. Berggren, G. Roos, H. van Houten, *Phys. Rev. B* 37 (1988) 10118.